Int. J. Electrochem. Sci., 15 **(2020)** 4005 – 4014, doi: 10.20964/2020.05.121

International Journal of
ELECTROCHEMICAL
SCIENCE
www.electrochemsci.org

Short Communication

Effect of the Electrodeposition Potential of Platinum on the Catalytic Activity of a Pt/GC Catalyst Toward Formic Acid Electro–Oxidation

Islam M. Al-Akraa [1,*], *Bilquis Ali Al-Qodami*[2], *Ahmad M. Mohammad* [2,*]

[1] Department of Chemical Engineering, Faculty of Engineering, The British University in Egypt, Cairo 11837, Egypt
[2] Chemistry Department, Faculty of Science, Cairo University, Cairo 12613, Egypt
[*]E-mails: islam.ahmed@bue.edu.eg (Islam M. Al-Akraa), ammohammad@cu.edu.eg (Ahmad M. Mohammad)

Received: 10 October 2019 / *Accepted:* 9 December 2019 / *Published:* 10 April 2020

The electrocatalytic activity of platinum (Pt)–modified glassy carbon (GC) (referred as Pt/GC) electrodes toward the formic acid electro–oxidation (FAO) was investigated. The Pt deposition on the GC substrate was carried out by a potentiostatic technique at different potentials (from 0.2 V to −0.2 V vs. $Hg/Hg_2Cl_2/KCl$ (sat.) reference electrode) and the corresponding influence on the catalytic activity toward FAO was monitored. The electrocatalytic inspection revealed a potential role for the Pt deposition potential in boosting the catalytic efficiency of the catalyst toward FAO and further in mitigating the CO poisoning that eventually deactivate the catalyst. Interestingly, the highest activity toward FAO was obtained at the Pt/GC electrode for which Pt was electrodeposited at 0.05 V. This was reflected from its high I_p^d/I_p^{ind} (20) and I_p^d/I_b (0.83) ratios that were employed to assess the electrocatalytic performance of the catalyst.

Keywords: Formic acid electro–oxidation; Pt nanoparticles; Electrodeposition potential; Fuel cells.

1. INTRODUCTION

The global energy crisis has stimulated a sincere effort to secure alternative clean abundant power supplies equivalent to the rapid increase in the world population [1-9]. In this regard, polymer electrolyte membrane fuel cells (PEMFCs) have attracted a growing interest in the replacement of batteries in portable power devices [1, 2]. Generally, fuel cells (FCs) which looks like galvanic batteries but reactants are continuously fed represent an essential element in the storage/restoring mechanisms of most renewable power plants.

Owing to their unique characteristics of enhanced efficiency, low price, reliability, robustness, safety, moving flexibility, low emissions (clean energy), long lasted, easily installed and noiselessness, FCs are currently supplying electricity for a variety of stationary, portable and backup electronic applications [10-13].

The criteria of selecting a specific fuel for FCs involves the nature, cost, toxicity, availability, security, calorific value, degradability, purity, water content, fuel cell performance, energy density selection of this fuel. In this regard, formic acid (FA) excelled much hydrogen "typical fuel" and methanol in PEMFCs making the fundamental research on the FA electro−oxidation (FAO) and the direct formic acid fuel cells (DFAFCs) attractive [3, 4, 14-18]. However, DFAFCs encounters a critical challenge decaying dramatically the catalytic activity of the Pt anodes that usually used for FAO. This originates from the "non-faradaic" dissociation of FA to CO that gets adsorbed strongly at the Pt surface; deteriorating ultimately the overall performance of DFAFCs [19-22]. Before going into marketing, the DFAFCs have to be durable and economic, which may not happen before overcoming the CO poisoning of the Pt catalyst.

In the last few century, the revolution in nanotechnology has facilitated the quick technological transfer of new developed nanomaterials of fascinating physical and chemical properties into real applications in electronics [23], water treatment [24], electrocatalysis and energy conversions [25, 26]. In particular, electrocatalysis by metal/metal oxide nanostructures has met diverse applications in electrochemistry because of their captivating properties that permitted their participation as catalytic mediators [8, 9, 27-29]. Doping/modifying the Pt surface with Au, Pd and NiOx nanostructures could to a great extent overcome the adsorption of poisoning CO and enhance the efficiency of FAO at low overpotentials [18, 30-32]. Replacing Pt with Pd, although appearing promising (providing a better activity toward FAO), ended up with a severe deactivation of the Pd catalyst [33-36]. That is why attention was renewed again in Pt–based materials regardless their comparatively lower catalytic activity.

In this study, the influence of the deposition potential of Pt nanoparticles on the catalytic activity of a Pt/CC electrode toward FAO was assessed and found important.

2. EXPERIMENTAL

2.1. Electrode's pretreatment and modification

A glassy carbon (d = 6.0 mm) electrode served as the working electrode. A saturated calomel electrode (SCE: $Hg/Hg_2Cl_2/KCl$ (sat.)) and a spiral Pt wire were used as the reference and counter electrodes, respectively. All potentials in this investigation, even if not mentioned, were recorded in reference to this calomel electrode. Conventional procedure was applied to clean the GC electrode as described previously [37].

A fixed amount (applied charge, Q = 2 mC) of Pt was electrodeposited on the bare GC from 0.1 M H_2SO_4 + 1.0 mM $K_2[PtCl]_6$ solution via a constant potential technique by holding the potential at − 0.20, − 0.10, − 0.05, 0.00, 0.05, 0.10 and 0.20 V vs. SCE. These potentials were identified from the

cyclic voltammogram (CV) of the Pt deposition in the same electrolyte between 1.0 and – 0.50 V vs. SCE according to the following electrochemical equation;

$$Pt^{4+} + 4e^{-} \rightarrow Pt \quad (1)$$

2.2. Electrochemical measurements

The electrochemical measurements were carried out in a traditional three-electrode glass cell at room temperature (~ 25 °C) using an EG&G potentiostat (model 273A) operated with Echem 270 software. The catalytic performance of the modified electrodes toward FAO was investigated in 0.3 M FA solution (pH = 3.5).

3. RESULTS AND DISCUSSION

3.1. Electrochemical characterization

Figure 1 shows the cyclic voltammogram (CV) of the GC electrode in 0.1 M H_2SO_4 + 1.0 mM $K_2[PtCl]_6$ solution at a scan rate of 20 mVs^{-1}. The potential scan started from 1.00 V to more negative potentials. The absence of the cathodic current at potentials more positive than 0.35 V reveals that the under potential deposition (UPD) in this system has not yet reached and that the electro-crystallization started in the overpotential deposition (OPD) region. This indicates a weak deposit-substrate interaction and recommends the Volmer-Weber growth mechanism for the deposition process [38, 39]. This growth mechanism works on electrodes with low surface energy as has been observed for the electrodeposition of metals on a GC substrate [39-41]. Further going cathodically (from 0.3 till – 0.3 V), the Pt deposition began followed by an intensive increase in the current due to the hydrogen adsorption and evolution which will be desorbed in the anodic sweep at ca. – 0.25 V. At a more positive potential (ca. 0.7 V), the oxidation peak assigns the oxidation of deposited Pt.

Based on the data of Fig. 1, the Pt deposition was planned to run potentiostatically onto the GC electrode at different potentials (E = – 0.20, – 0.10, – 0.05, 0.00, 0.05, 0.10 and 0.20 V) where Q is kept constant at 2.0 mC (Fig. 2). Figure 2 obviously classifies the entire range of deposition potentials into two domains intersecting at 0.05 V. All the Pt catalysts prepared at a more negative potential than 0.05 V showed early (in less than 5s) which perhaps correspond to the H_2 desorption at the Pt surface. This indicated that Pt was very quickly deposited on the GC surface in contrast to the Pt/GC catalysts prepared at higher potentials (> 0.05 V). The rate of Pt deposition is expected to influence the morphology and structure of Pt at the surface which can further affect its electronic properties and catalytic activity.

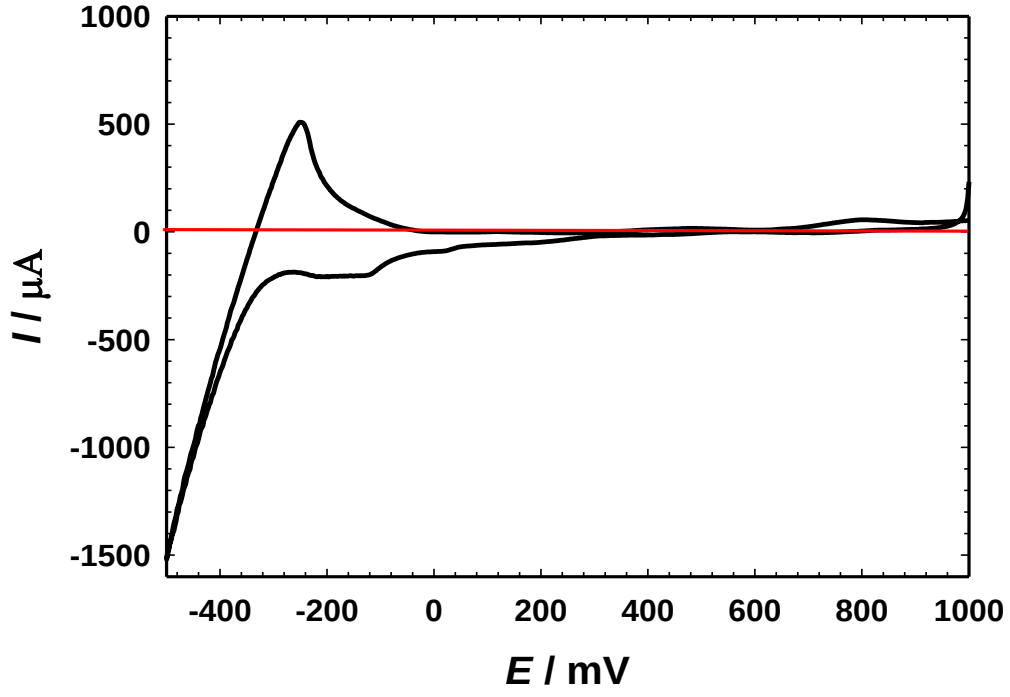

Figure 1. CV of GC electrode in 0.1 M H_2SO_4 + 1.0 mM $K_2[PtCl]_6$ solution at a scan rate of 20 mVs^{-1}.

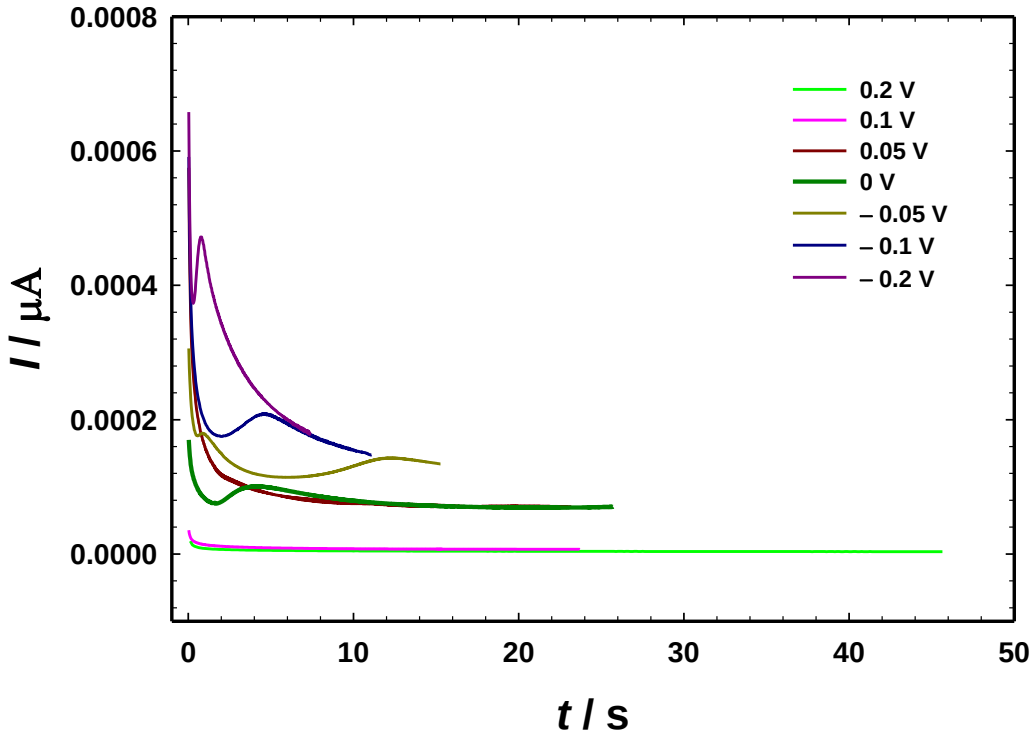

Figure 2. Current transients of GC electrode in 0.1 M H_2SO_4 + 1.0 mM $K_2[PtCl]_6$ solution at different Pt electrodeposition potentials (E = – 0.20, – 0.10, – 0.05, 0.00, 0.05, 0.10 and 0.20 V) where Q is kept constant at 2.0 mC.

By the way, we intended to inspect the role of the deposition potential of Pt at the various catalysts on their electrocatalytic activity toward FAO but with the application of the same charge (Q = 2.0 mC) to avoide the influence of the Pt mass. The various Pt/GC (with different Pt deposition potentials) catalysts were passed for an electrochemical characterization; the sensitive tool to confirm the Pt deposition. Figure 3 shows the characteristic CVs of the Pt/GC electrode at different Pt deposition potentials (E = – 0.20, – 0.10, – 0.05, 0.00, 0.05, 0.10 and 0.20 V) where Q is kept constant at 2.0 mC. At all electrodes, the characteristic behavior of polycrystalline Pt was clearly observed where the Pt oxidation extended over a wide range of potential (0.50 to 1.30 V) with its subsequent reduction (PtO→Pt) in the cathodic-going scan at ca. 0.30 V. In addition, the hydrogen adsorption/desorption peaks appeared in the potential range from 0.0 to – 0.2 V with intensities depending on the deposition potential of Pt .

3.2. Electrocatalysis of FAO

Figure 4 shows the CVs of FAO in 0.3 M formic acid (pH = 3.5) solution at different Pt electrodeposition potentials (E = – 0.20, – 0.10, – 0.05, 0.00, 0.05, 0.10 and 0.20 V) where Q is kept constant at 2.0 mC.

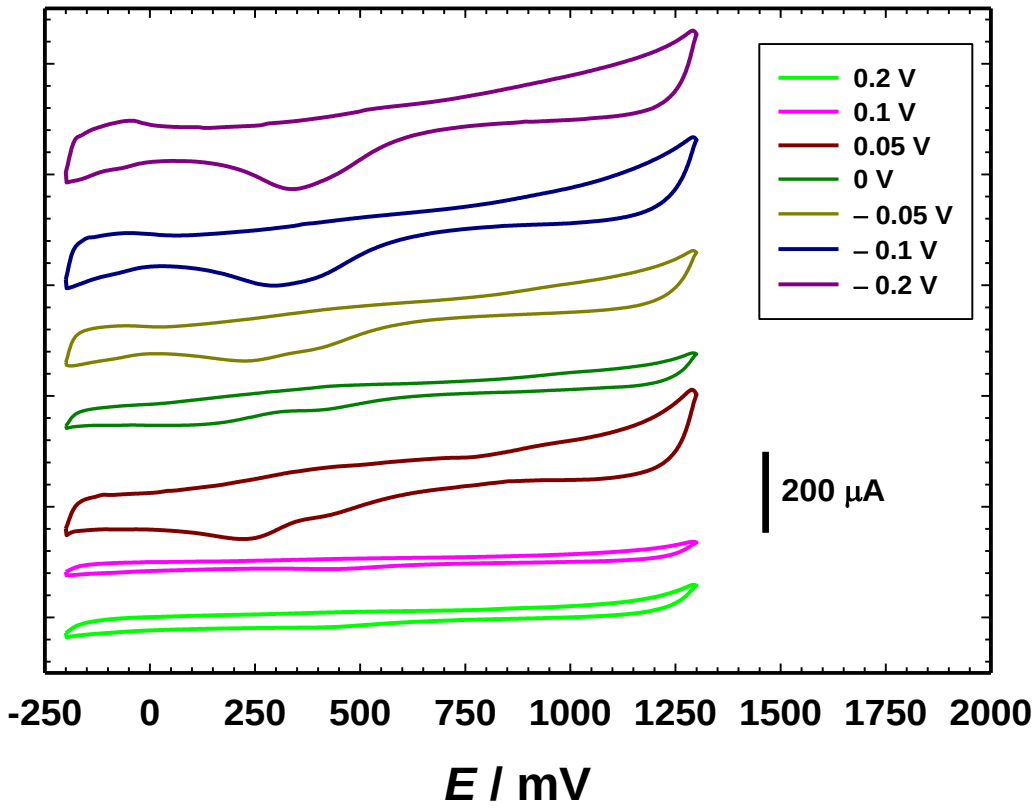

Figure 3. CVs obtained at the Pt/GC electrode in 0.1 M H_2SO_4 solution at different Pt electrodeposition potentials (E = – 0.20, – 0.10, – 0.05, 0.00, 0.05, 0.10 and 0.20 V) where Q is kept constant at 2.0 mC.

In fact, at Pt-based electrocatalysts, FAO proceeds in two different pathways at the same time [42, 43]. The first one involves dehydrogenation of FA to CO_2. This takes place at a low overpotential that makes the voltage output of DFAFCs closer to the theoretical value; hence, this is the desirable pathway for FAO. In Fig. 4, the peak observed at 0.3 V in the forward scan corresponds to the direct oxidation of FA to CO_2 (Eq. 2). The current of this peak (I_p^d) is used to assess the density of active Pt sites participating in the direct FAO.

$$HCOOH_{(aq)} + Pt \rightarrow Pt + CO_{2(g)} + 2H^+_{(aq)} + 2e^- \quad (2)$$

At the same time, FA can be non-faradiacally dissociated at open circuit potential to produce CO (Eq. 3) that get strongly adsorbed on the Pt surface to deactivate a large portion from the Pt sites against the participation in FAO.

$$HCOOH + Pt \rightarrow Pt\text{–}CO_{ads} + H_2O \quad (3)$$

At higher overpotentials later after hydroxylating the Pt surface, the poisoning CO is oxidized again to CO_2 and the peak observed at ca. 0.6 V in the forward scan corresponds to this indirect oxidation pathway. Here, the current of this peak (I_p^{ind}) may provide an idea about the intensity of CO poisoning at the Pt surface.

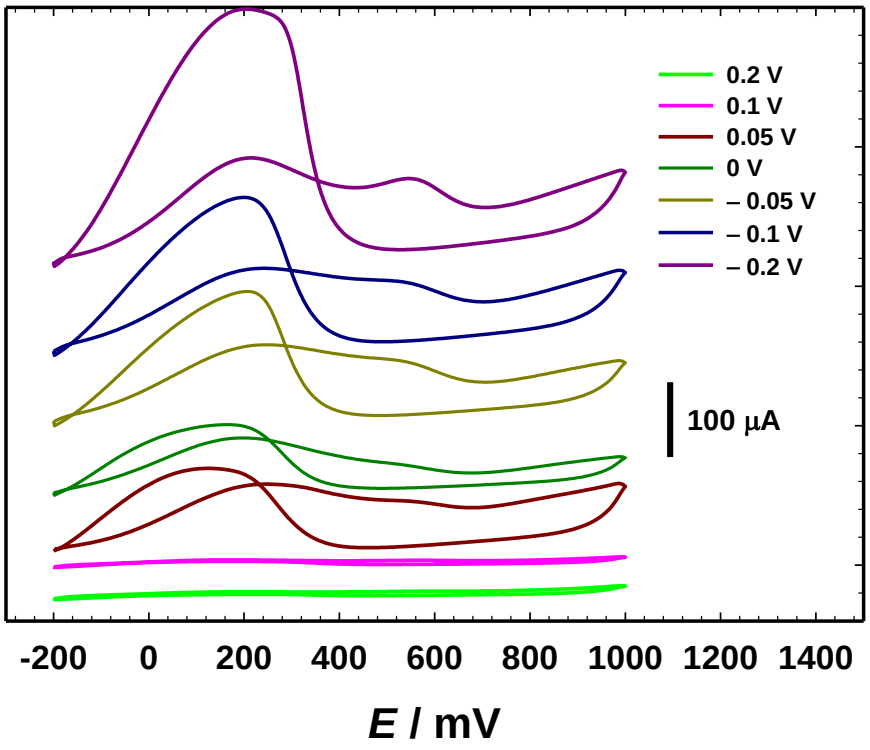

Figure 4. CVs of FAO in 0.3 M formic acid (pH = 3.5) solution at different Pt electrodeposition potentials (E = – 0.20, – 0.10, – 0.05, 0.00, 0.05, 0.10 and 0.20 V) where Q is kept constant at 2.0 mC.

In the backward scan (cathodic scan), after the oxidation of most poisoning CO in the forward scan, FAO proceeded mainly via the direct pathway (look at the peak around 0.2 V in the backward cathodic scan and its corresponding current, I_p^b).

The relative ratios of I_p^d/I_p^{ind} and I_p^d/I_p^b were calculated to quantify the degree of catalytic enhancement and the decrease of CO poisoning, respectively, during FAO at the prepared electrodes. Table 1 shows the I_p^d/I_p^{ind} and I_p^d/I_p^b ratios for all prepared electrodes in comparison to previous cited values for similar catalysts. It is worth to mention that the response of FAO for the electrodes at which Pt deposited at 0.10 and 0.20 V was very weak as shown in Fig. 4 (this matches with their characteristics behavior in Fig. 3) and so we excluded them from the further inspection. As Table 1 indicates, the potentiostatic electrodeposition of Pt at fixed potentials (from 0.05 V to – 0.20 V as was done in this investigation) exhibited the highest catalytic activities if compared to previous results for bare Pt or even Pt/GC (Pt was deposited by potential step electrolysis) catalysts. Interestingly, moreover, within the deposition potentials employed, the highest I_p^d/I_p^{ind} and I_p^d/I_p^b ratios were obtained at the Pt/GC electrode for which the Pt was electrodeposited at 0.05 V. This might originate due to some morphological and/or structural influences (under investigation in our laboratory) that perhaps enriched the Pt surface in the preferred orientation for FA adsorption and/or in the way weakening the Pt–CO bonding [31, 44-48].

Table 1. A summary of the I_p^d / I_p^{ind} and I_p^d / I_p^b ratios for all prepared electrodes (summarized from Fig. 4) in comparison to other data from literature.

E of Pt deposition / V	Catalyst	I_p^d / I_p^{ind}	I_p^d / I_p^b	*Ref.*
0.05	Pt/GC	20	0.83	This work
0.00	Pt/GC	19	0.83	This work
– 0.05	Pt/GC	15	0.58	This work
– 0.10	Pt/GC	12	0.50	This work
– 0.20	Pt/GC	6	0.38	This work
Potential step electrolysis from 1 to 0.1 V	Pt/GC	2	0.20	[49]
Bare Polycrystalline Pt electrode	Pt	2.3	0.31	[50]
Bare Pt substrate	Pt	0.6	0.2	[51]

4. CONCLUSION

The Pt deposition onto the GC electrode was carried out by a potentiostatic technique at different potentials. Electrochemical investigations confirmed that the Pt deposition at a potential of 0.05 V resulted the highest catalytic activity toward FAO with the highest I_p^d/I_p^{ind} (20) and I_p^d/I_p^b (0.83) ratios; indicating the highest activity toward the direct FAO and the best tolerance toward CO poisoning, respectively. This is thought to a consequent change in the particle size, distribution, and/or crystallographic orientation of the deposited Pt due to the deposition potential change.

ACKNOWLEDGEMENT
This research was supported from the General Scientific Research Department of Cairo University, Egypt (Grant 77/2016).

References

1. A. Boddien, D. Mellmann, F. Gärtner, R. Jackstell, H. Junge, P. J. Dyson, G. Laurenczy, R. Ludwig, M. Beller, *Science*, 333 (2011) 1733.
2. C. Li, Q. Yuan, B. Ni, T. He, S. Zhang, Y. Long, L. Gu, X. Wang, *Nat. Commun.*, 9 (2018) 3702.
3. I. M. Al-Akraa, A. M. Mohammad, M. S. El-Deab, B. S. El-Anadouli, *Int. J. Electrochem. Sci.*, 10 (2015) 3282.
4. I. M. Al-Akraa, *Int. J. Hydrogen Energy*, 42 (2017) 4660.
5. F. Xia, S. E. C. Dale, R. A. Webster, M. Pan, S. Mu, S. C. Tsang, J. M. Mitchels, F. Marken, *New J Chem*, 35 (2011) 1855.
6. N. Cheng, H. Lv, W. Wang, S. Mu, M. Pan, F. Marken, *J. Power Sources*, 195 (2010) 7246.
7. N. Cheng, R. A. Webster, M. Pan, S. Mu, L. Rassaei, S. C. Tsang, F. Marken, *Electrochim. Acta*, 55 (2010) 6601.
8. I. M. Al-Akraa, T. Ohsaka, A. M. Mohammad, *Arab. J. Chem.*, 12 (2019) 897.
9. I. M. Al-Akraa, A. M. Mohammad, M. S. El-Deab, B. E. El-Anadouli, *Arab. J. Chem.*, 10 (2017) 877.
10. M. K. Debe, *Nature*, 486 (2012) 43.
11. Y. Wang, K. S. Chen, J. Mishler, S. C. Cho, X. C. Adroher, *Appl. Energy*, 88 (2011) 981.
12. R. Borup, J. Meyers, B. Pivovar, Y. S. Kim, R. Mukundan, N. Garland, D. Myers, M. Wilson, F. Garzon, D. Wood, P. Zelenay, K. More, K. Stroh, T. Zawodzinski, J. Boncella, J. E. McGrath, M. Inaba, K. Miyatake, M. Hori, K. Ota, Z. Ogumi, S. Miyata, A. Nishikata, Z. Siroma, Y. Uchimoto, K. Yasuda, K. I. Kimijima, N. Iwashita, *Chem. Rev.*, 107 (2007) 3904.
13. B. C. H. Steele, A. Heinzel, *Nature*, 414 (2001) 345.
14. Y. M. Asal, I. M. Al-Akraa, A. M. Mohammad, M. S. El-Deab, *Int. J. Hydrogen Energy*, 44 (2019) 3615.
15. Y. M. Asal, I. M. Al-Akraa, A. M. Mohammad, M. S. El-Deab, *J. Taiwan Inst. Chem. Eng.*, 96 (2019) 169.
16. I. M. Al-Akraa, Y. M. Asal, A. M. Mohammad, *J. Nanomater.* , 2019 (Article ID 2784708) (2019): https://doi.org/10.1155/2019/2784708.
17. A. M. Mohammad, I. M. Al-Akraa, M. S. El-Deab, *Int. J. Hydrogen Energy*, 43 (2018) 139.
18. I. M. Al-Akraa, A. M. Mohammad, M. S. El-Deab, B. E. El-Anadouli, *J. Electrochem. Soc.*, 162 (2015) F1114.
19. H. Lee, S. E. Habas, G. A. Somorjai, P. Yang, *J. Am. Chem. Soc.*, 130 (2008) 5406.
20. S. Y. Uhm, S. T. Chung, J. Y. Lee, *Electrochem. Commun.*, 9 (2007) 2027.

21. N. M. Markovic, H. A. Gasteiger, P. N. R. Jr., X. Jiang, I. Villegas, M. J. Weaver, *Electrochim. Acta*, 40 (1995) 91.
22. G. A. El-Nagar, A. M. Mohammad, M. S. El-Deab, T. Ohsaka, B. E. El-Anadouli, *J. Power Sources*, 265 (2014) 57.
23. A. M. Mohammad, S. Dey, K. K. Lew, J. M. Redwing, S. E. Mohney, *J. Electrochem. Soc.*, 150 (2003) G577.
24. A. M. Mohammad, T. A. Salah Eldin, M. A. Hassan, B. E. El-Anadouli, *Arab. J. Chem.*, 10 (2017) 683.
25. G. A. El-Nagar, M. S. El-Deab, A. M. Mohammad, B. E. El-Anadouli, *Electrochimica Acta*, 180 (2015) 268.
26. I. M. Sadiek, A. M. Mohammad, M. E. El-Shakre, M. S. El-Deab, B. E. El-Anadouli, *Journal of Solid State Electrochemistry*, 17 (2013) 871.
27. I. M. Al-Akraa, A. M. Mohammad, M. S. El-Deab, B. E. El-Anadouli, *Int. J. Electrochem. Sci.*, 8 (2013) 458.
28. I. M. Al-Akraa, Y. M. Asal, A. M. Arafa, *Int. J. Electrochem. Sci.*, 13 (2018) 8775.
29. I. M. Al-Akraa, Y. M. Asal, S. D. Khamis, *Int. J. Electrochem. Sci.*, 13 (2018) 9712.
30. I. M. Al-Akraa, A. M. Mohammad, M. S. El-Deab, B. E. El-Anadouli, *Int. J. Hydrogen Energy*, 40 (2015) 1789.
31. I. M. Al-Akraa, A. M. Mohammad, M. S. El-Deab, B. S. El-Anadouli, *International Journal of Electrochemical Science*, 10 (2015) 3282.
32. I. M. Al-Akraa, A. M. Mohammad, M. S. El-Deab, B. E. El-Anadouli, *Int. J. Electrochem. Sci.*, 7 (2012) 3939.
33. S. M. Baik, J. Han, J. Kim, Y. Kwon, *Int. J. Hydrogen Energy*, 36 (2011) 14719.
34. C. Rice, S. Ha, R. I. Masel, A. Wieckowski, *J. Power Sources*, 115 (2003) 229.
35. W. S. Jung, J. Han, S. Ha, *J. Power Sources*, 173 (2007) 53.
36. S. D. Han, J. H. Choi, S. Y. Noh, K. Park, S.K.Yoon, Y. W. Rhee, *Korean J. Chem. Eng.*, 26 (2009) 1040.
37. M. S. El-Deab, G. H. El-Nowihy, A. M. Mohammad, *Electrochim. Acta*, 165 (2015) 402.
38. A. E. ALvarez, D. R. Salinas, *Electrochim. Acta*, 55 (2010) 3714.
39. L. Komsiyska, G. Staikov, *Electrochim. Acta*, 54 (2008) 168.
40. S. M. El-Refaei, G. A. El-Nagar, A. M. Mohammad, B. E. El-Anadouli, in *Progress in Clean Energy, Volume 1: Analysis and Modeling*. (Springer International Publishing, 2015), pp. 595-604.
41. G. A. El-Nagar, A. M. Mohammad, M. S. El-Deab, B. E. El-Anadouli, in *Progress in Clean Energy, Volume 1: Analysis and Modeling*. (Springer International Publishing, 2015), pp. 577-594.
42. R. Larsen, S. Ha, J. Zakzeski, R. I. Masel, *J. Power Sources*, 157 (2006) 78.
43. J. D. Lović, A. V. Tripković, S. L. J. Gojković, K. D. Popović, D. V. Tripković, P. Olszewski, A. Kowal, *J. Electroanal. Chem.*, 581 (2005) 294.
44. W. H. Qi, M. P. Wang, *J. Nanopart. Res.*, 7 (2005) 51.
45. M. Rezaei, S. H. Tabaian, D. F. Haghshenas, *Electrochim. Acta*, 59 (2012) 360.
46. P. Kalimuthu, S. A. John, *J. Electroanal. Chem.*, 617 (2008) 164.
47. N. Hoshi, M. Nakamura, K. Kida, *Electrochem. Commun.*, 9 (2007) 279.
48. L. Zhang, Q. Sui, T. Tang, Y. Chen, Y. Zhou, Y. Tang, T. Lu, *Electrochem. Commun.*, 32 (2013) 43.
49. M. S. El-Deab, G. A. El-Nagar, A. M. Mohammad, B. E. El-Anadouli, *J. Power Sources*, 286 (2015) 504.
50. B. A. Al-Qodami, H. H. Farrag, S. Y. Sayed, N. K. Allam, B. E. El-Anadouli, A. M. Mohammad, *J. Nanotechnol.*, 2018 (Article ID 4657040) (2018): https://doi.org/10.1155/2018/4657040.

51. I. M. Al-Akraa, A. M. Mohammad, *Arab. J. Chem.*, in Press (2019): https://doi.org/10.1016/j.arabjc.2019.10.013.